Nonlinear development of lower hybrid cones

N. R. Pereira

Lawrence Berkeley Laboratory, University of California, Berkeley, California 94720

A. Sen and A. Bers

Research Laboratory of Electronics and Plasma Fusion Center, Massachusetts Institute of Technology, Cambridge, Massachusetts 02139
(Received 8 August 1977)

The instability of a planar lower hybrid soliton to transverse long wavelength perturbations is investigated numerically. Initially, a kink-like deformation grows in agreement with linear analysis. In the nonlinear regime the soliton breaks up into bunches which move apart and spread the energy throughout the plasma.

I. INTRODUCTION

Self-modulation effects are thought to be important for the nonlinear evolution of lower hybrid resonance cones which have been excited at the wall of the plasma chamber by a finite extent source such as a phased waveguide array or a slow wave structure.[1-3] Since self-modulation usually leads to self-focusing or filamentation, the primary concern has been to examine whether these effects would impede the propagation of rf energy into the interior of the plasma. Depending on the initial assumptions about the nature of the excitation spectrum, the nonlinear equation governing the propagation of the lower hybrid waves is the modified Korteweg de-Vries equation[1] or the nonlinear Schrödinger equation.[2,3] Most derivations of these equations restrict analysis to the plane containing the ambient magnetic field and the electric field of the pump wave,[1,2] and associate planar stationary solutions of the soliton kind with filamentation effects. In Ref. 3 the effect of including the third dimension was studied, and it was shown that such planar structures were linearly unstable to long wavelength transverse perturbations and that the tendency of the cones to filament was opposed by additional dispersive terms.

In this paper we numerically verify the analytic results of the linear stability analysis and in addition, examine the nonlinear evolution of the resonance cone structures. The pertinent equation is the nonlinear Schrödinger equation with an additional term [Eq. (26) of Ref. 3]

$$i\frac{\partial v}{\partial \tau}+\frac{\partial^2 v}{\partial \xi^2}-\frac{\partial^2 v}{\partial \eta^2}+2|v|^2 v=0, \tag{1}$$

where v is the normalized electrostatic field amplitude $\epsilon_0^{1/2}k_{1x}\phi/(4nT)^{1/2}$. The derivation of this equation, the validity assumptions, and the physical meaning are detailed in Ref. 3. We will describe its physical content here. Basically, the equation describes the evolution of the slowly varying envelope of a monochromatic lower hybrid wave whose potential is $\phi(x)\exp(-i\omega t)$. The potential is further expressed as $\phi(\tau,\xi,\eta)\exp(ik_z z - ik_x x)$ where the slowly varying envelope ϕ is a function of the stretched variables τ, ξ, and η. The geometry of the problem is sketched in Fig. 1 where the orientations of the coordinates ξ and η are shown in relation to the basic resonance cone structure in the $x-z$ plane. $\partial/\partial\xi$ and $\partial/\partial\eta$ characterize the slow envelope variation in the $x-z$ plane and y direction, respectively, in the absence of the weak effects of nonlinearity and dispersion, whereas $\partial/\partial\tau$ describes the perturbation to the envelope due to nonlinearity and dispersion. This perturbation is along the x direction, or the minor radial direction in a toroidal geometry. Thus, in the present problem the evolution in the time-like variable τ corresponds to evolution along x.

We note that Eq. (1) differs from the usual nonlinear Schrödinger equation by the presence of the additional term $\partial^2 v/\partial\eta^2$ which arises from inclusion of slow variations in the third dimension. The negative sign preceding this term sets our equation apart from the Langmuir wave equation which has a positive sign.[4,5] The sign difference can be traced to the physical origin of the two dispersive terms: The $\partial^2/\partial\xi^2$ term arises from

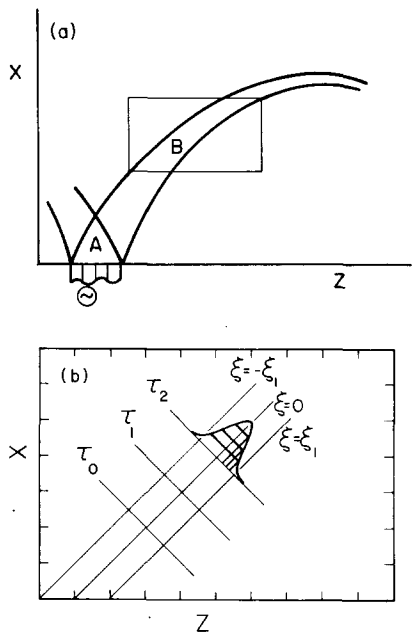

FIG. 1. (a) Lower hybrid resonance cone for a typical case. Region A contains electromagnetic waves, region B electrostatic lower hybrid waves. The scales of x and z are arbitary. (b) Expanded and simplified picture of region B. The coordinates ξ and τ are perpendicular to each other and the coordinate η is normal to the plane of the figure. The location of the energy density at τ_2 is indicated by the shaded soliton shape. Some contour lines are also shown.

 0031-9171/78/2101-0117$00.90

thermal corrections to the cold propagation characteristics of the lower hybrid wave and is proportional to k_x whereas the $\partial^2/\partial\eta^2$ term is nonthermal in origin and represents the spreading out of the wave in a three-dimensional cone centered about the excitation source. For the nonlinear Langmuir wave equation both the terms arise from thermal corrections which are proportional $k_\perp$ and hence in terms of k_x and k_y the positive sign appears. In our case k_y is set to zero and only slow variations in y are retained. The asymmetry in ξ and η of Eq. (1), due to the negative sign, has significant effects on the nonlinear structure of the solutions which evolve quite differently from those of the Langmuir wave case.

The plan of our paper is as follows: In Sec. II we present the numerical results for the linear evolution of a transverse perturbation to a planar soliton solution of Eq. (1) and compare these to analytical estimates.[6,3] In Sec. III the perturbation is followed in the nonlinear regime until extraneous factors arising from limitations of the numerical scheme begin to develop. A comparison is made with previous investigations of the closely related equation for the Langmuir waves. Our results are summarized and their implications for lower hybrid heating schemes are briefly discussed in the final section.

II. LINEAR INSTABILITY

In this section we present numerical results for the linear instability of a planar sech-shaped lower hybrid soliton perturbed in the perpendicular direction. The computations were performed with a variant of the code used earlier to study strong Langmuir turbulence,[5] which is described by Eq. (1) with a plus sign in front of the η derivative. We used a grid of 32×32 points with 334 Fourier modes. The accuracy of the computations was checked by repeating some of them with different grid sizes and time steps; the results were only slightly influenced. In addition, the conserved integral $\int |v|^2 d\xi\, d\eta$ remained constant to a high accuracy.

For a planar soliton of the form $v_0 = \mathrm{sech}(\xi)$ perturbations even in ξ are found to be stable in the computations; this is in agreement with the analytical calculations[6,7,3] and the computations are not shown here. The instability of a planar soliton to perturbations odd in ξ, of the form

$$\delta v(\xi, \eta, \tau) = a(0)(\partial v_0/\partial\xi)\cos(\kappa\eta), \tag{2}$$

is shown in Figs. 2(a), (b), and (c) for $\tau=0$, $\tau=4$, and $\tau=6$, respectively. The perturbation wavelength is equal to the periodicity length in the η direction of our system and the initial amplitude is $a(0)=0.1$. The perturbation appears as a kink-like deformation of a planar soliton, since (2) is the first term in a Taylor series of the bent sech-shaped soliton $v=\mathrm{sech}[\xi + a\cos(\kappa\eta)]$, which has its maximum along the line $\xi = -a\cos(\kappa\eta)$. Because the initial amplitude is chosen to be very small, these kinks do not yet show up in Fig. 2(a).

At $\tau=4$, Fig. 2(b), the amplitude of the kinks has increased according to the linear growth rate, but the

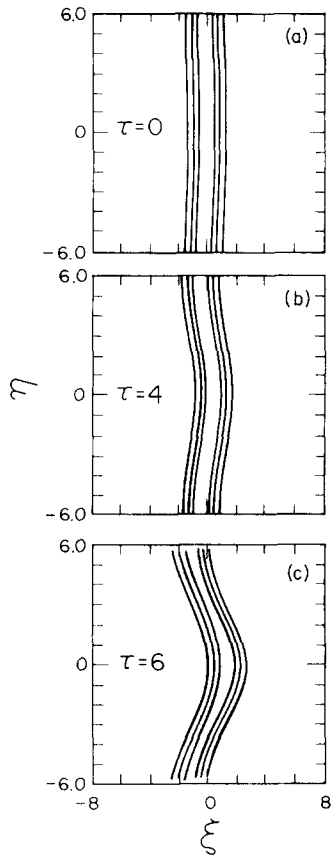

FIG. 2. The electrostatic energy density $|v|^2(\xi,\eta)$ for a soliton normalized to unity with perpendicular wave number $\kappa=\pi/6$. The lines are the contours at 0.75, 0.5 and 0.25.

height of the soliton has only changed slightly. At $\tau=6$, Fig. 1(c), the soliton starts to deviate from linear growth. The profile along a line $\eta=$ const is different from the initial shape, and the height is now clearly modulated along a line through the soliton maxima.

We note that Fig. 2 corresponds closely to the theoretical calculations of Yajima.[7] He assumes a solution of the form

$$v = A(\eta,\tau)\,\mathrm{sech}\{A(\eta,\tau)[\xi + \xi_0(\eta,\tau)]\},$$

and finds that a sinusoidal perturbation in η on the position of the maximum ξ_0 grows with the growth rate given in (3). Sinusoidal perturbations on height and inverse width $A(\eta,\tau)$ can oscillate in time, in agreement with numerical computations that are not shown.

We now compare the observed linear growth rate with earlier analytic results. From Ref. 3 the linear growth rate is

$$\Gamma^2 \simeq \tfrac{4}{3}\kappa^2 - 1.02\kappa^4 + O(\kappa^6). \tag{3}$$

The solid line in Fig. 3 represents the calculated growth rate (3). The dots are results from the computations, obtained by measuring the τ behavior of the maximum value $m(\tau)$ of the perturbed minus the unperturbed soliton

$$m(\tau) = [\,|v(\xi,\eta,\tau)|^2 - |v(\xi,\eta,\tau=0)|^2]_{\max} \simeq a(\tau)\left.\frac{\partial|v|^2}{\partial\xi}\right|_{\max}. \tag{4}$$

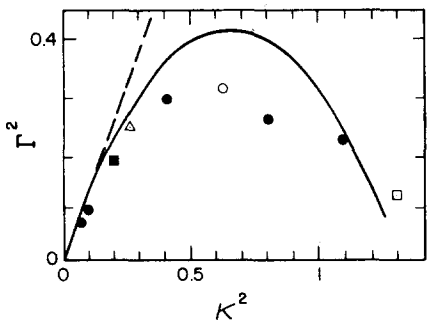

FIG. 3. The square of the growth rate Γ^2 as a function of the square of the perpendicular wavenumber κ^2. The solid line is Eq. (3). The cross corresponds to the computation of Fig. 2 with $\kappa = \pi/6$, the open circle corresponds to Fig. 6 with $\kappa = \pi/4$, and the dots and squares to other computations.

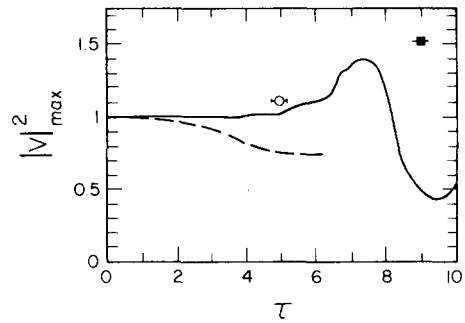

FIG. 5. The time dependence of the electrostatic energy density maximum, $|v|^2_m$, from the computation of Figs. 2 and 4 with $\kappa = \pi/6$. The open circle is the maximum in time of $|v|^2_m$ for $\kappa = \pi/4$ shown in Fig. 6; the solid square is for $\kappa = \pi/7$.

The logarithm of $m(\tau)$ is plotted versus τ, and the slope of the straight portion of this plot yields the growth rate. For perpendicular wavenumbers κ of about 0.25–0.5, that is, much smaller than unity but not too small, we find exponential growth over a sizeable range of τ, and the determination of the growth rate is reasonably accurate. For values of κ outside this range the exponential growth in τ is smaller, and the numerical growth rate is less accurate. From Fig. 3 we see that the growth rate from the numerical computations, as represented by the dots, follows the theoretical curve quite well, up to $\kappa^2 = 0.3$. The growth rate is proportional to κ for small κ, and within our numerical accuracy the proportionality constant is close to the theoretical value of $\sqrt{4/3}$. For larger κ the growth rate reaches a maximum, and for still larger κ it decreases following once again the qualitative behavior of the theoretical curve. The maximum growth is about 0.3 or 0.75 of the value suggested by (3), and it occurs near the predicted value of κ^2 of 0.67. For larger κ the growth rate decreases more slowly than that predicted by (3). However, these cases do not show the clear kinks visible in Fig. 2(c) because the nonlinear growth sets in at an early stage.

The linear development of the instability changes to a nonlinear stage at larger τ when the amplitude of the growing odd perturbation has reached about 0.5 of the unperturbed planar soliton. Then, the absolute values of maximum and minimum of the perturbation, which remain equal in the linear stage, begin to differ appreciably. This nonlinear development is treated in the next section.

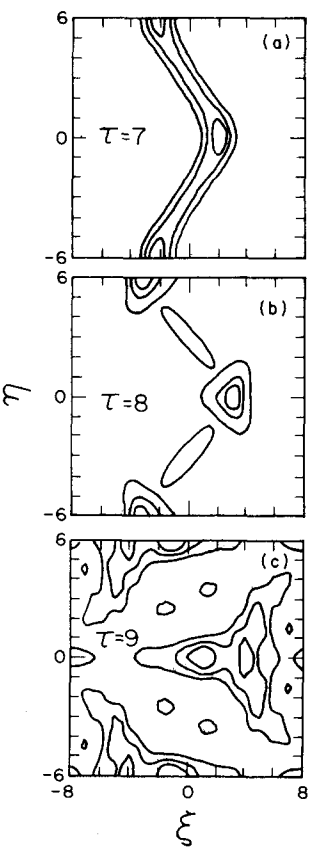

FIG. 4. The electrostatic energy density for the computations of Fig. 2 at later times.

III. NONLINEAR DEVELOPMENT

In the nonlinear regime there are no analytic predictions of the final state of the lower hybrid waves as described by Eq. (1), and we therefore investigate this state numerically by following the development of the kink-like instability well beyond its linear stage.

Figures 4(a), (b), and (c) picture the evolution of the same soliton as in Fig. 2 for $\tau = 7$, $\tau = 8$, and $\tau = 9$, respectively. Now, the perturbation of the soliton is not a pure modulation of the position of the soliton maximum, but this maximum and the corresponding width vary along the soliton ridge and with τ. Depending on the perturbation wavenumber, the soliton maximum can obtain values up to twice the initial maximum: the soliton of Fig. 4 reaches 1.4 times the initial maximum at $\tau = 7.3$. Subsequently, as in Fig. 4(b), the soliton breaks up into pieces which cannot keep themselves together but instead spread out.

In contrast to the Langmuir problem, where the final state is a self-similarly contracting blob of energy density leading to a rapid increase of energy density to infinity in a finite time (collapse), the energy density in this case remains bounded at all times. The energy density maximum versus time of the soliton of Figs. 2 and 4 is plotted in Fig. 5. The maximum oscillates slightly, and in addition increases slowly toward the

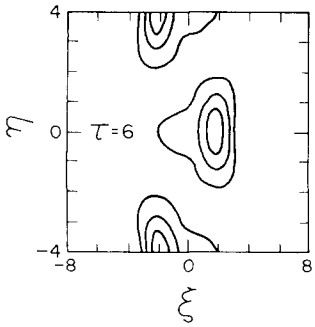

FIG. 6. The electrostatic energy density $|v|^2$ for $\kappa = \pi/4$ at $\tau = 6$. Note the change of scale in the η direction.

end of the linear growth at $\tau = 6$. This growth accelerates in the nonlinear regime, until at $\tau = 7.3$ the largest value 1.4 is reached. Afterwards, the maximum decreases rapidly since at this time the soliton begins to disperse in ξ and η.

The upturn after $\tau = 9.5$ is related to the interference pattern seen in Fig. 4(c), which does not, however, represent the end stage of a single decaying soliton. Namely, our computations take place in a doubly periodic system and therefore as the instability progresses the soliton moves toward the boundary of its period, where it gets close to the soliton of the next period. Interference between these solitons then results in pictures like Fig. 4(c). In this interference process the maximum reaches larger values than the minimum shown in Fig. 5, but we have not observed values larger than the initial value. This situation of Fig. 4(c) is spurious in the present computation, which intends to treat one soliton only, but it could correspond closely to a heating scheme where the lower hybrid waves are launched through multiple ports placed around the torus of a tokamak. Physically adjacent resonance cones could then simulate such a situation.

The energy density maximum in space and time for values adjacent to $\kappa = \pi/6$, namely, $\kappa = \pi/4$ and $\kappa = \pi/7$, is indicated in Fig. 5 by the open circle and the closed square. The maximum takes place later when the wavenumber is smaller, in agreement with the smaller growth rate. The value of the maximum is a decreasing function of the wavenumber. We do not know of a quantitative theory that relates the value and occurrence of this maximum to the perpendicular wavenumber. Such a theory would undoubtedly be very difficult, and we have not tried to construct one in view of our limited objectives. Qualitatively, it seems clear that the maximum occurs when the kinks become substantial.

The dashed line in Fig. 5 shows the maximum energy density versus time for $\kappa = \pi/2.75$ corresponding to the open square in Fig. 3. After the short linear stage the soliton maximum does not increase, but instead decreases until the end of this computation at $\tau = 6$. Indeed, this soliton never shows the clearly visible kinks of Figs. 2 and 4, but has slightly oscillating kinks that decay from the beginning.

In practice, instabilities often develop from random perturbations and the one with the largest growth rate will eventually dominate. Figure 6 shows the soliton with this fastest growing perturbation with $\kappa^2 = 0.5$ at $\tau = 6$. This and other computations exhibit, qualitatively, the same behavior as illustrated in Figs. 2 and 4.

IV. SUMMARY

We have investigated the linear and nonlinear instability of a planar soliton subjected to a long wavelength transverse perturbation. Such an instability is related to the nonlinear evolution of lower hybrid resonance cones as described by Eq. (1), which takes into account the nonlinear effects of self-modulation and the perturbative effects of dispersion of the cones in the third dimension.

In the linear regime our computations agree with the analytic results quite well. We have further investigated the nonlinear stage of this instability and found that the soliton eventually breaks up into smaller pieces which cannot keep themselves together but spread out. This is in contrast to the final collapse state in the Langmuir wave equation,[8,5] which is identical to Eq. (1) except for the sign of the second dispersive term.

For the lower hybrid cones, therefore, the nonlinear evolution in the presence of self-modulation can be described as follows. Initially, a kink-like instability with perpendicular wavenumber in the linearly most unstable regime around $\kappa = 0.5$ will grow and distort the cone. During the process the maximum of the energy density may reach values up to 1.5 times the initial energy density. Subsequent nonlinear development causes the energy to spread throughout the plasma[3] rather than being focused into small regions.

ACKNOWLEDGMENTS

We acknowledge many helpful discussions with C. F. F. Karney and valuable comments from A. N. Kaufman.

The computations were performed at the National Magnetic Fusion Energy Computing Center, Livermore, California.

This work was supported by the National Science Foundation (Grant No. ENG 75-06242) and by the U.S. Energy Research and Development Administration (Contracts No. EX-76-A-01-2295 and W-7405-ENG-48).

[1]G. J. Morales and Y. C. Lee, Phys. Rev. Lett. **35**, 930 (1975).
[2]H. H. Kuehl, Phys. Fluids **19**, 1972 (1977).
[3]A. Sen, C. F. F. Karney, G. L. Johnston, and A. Bers, Massachusetts Institute of Technology Research Laboratories of Electronics Report RLE-PRR 77-16 (1977).
[4]V. E. Zakharov, Zh. Eksp. Teor. Fiz. **62**, 1745 (1972) [Sov. Phys.-JETP **35**, 908 (1972)].
[5]N. R. Pereira, R. N. Sudan, and J. Denavit, Phys. Fluids **20**, 936 (1977).
[6]V. E. Zakharov and A. M. Rubenchik, Zh. Eksp. Teor. Fiz. **65**, 997 (1973) [Sov. Phys.-JETP **38**, 494 (1974)].
[7]N. Yajima, Prog. Theor. Phys. Jpn. **52**, 1066 (1974).
[8]L. M. Degtyarev and V. E. Zakharov, Zh. Eksp. Teor. Fiz. Pis'ma Red. **20**, 365 (1974) [JETP Lett. **20**, 164 (1974)]; L. M. Degtyarev, V. E. Zakharov, and L. I. Rudakov, Fiz. Plasmy **2**, 438 (1976) [Sov. J. Plasma Phys. **2**, 240 (1977)].